

## Micro- and nanocrystals of the iron(III) spin-transition material $[\text{Fe}^{\text{III}}(\text{3-CH}_3\text{O-SalEen})_2]\text{PF}_6$ .

Antoine Tissot, Lionel Rechinat, Azzedine Bousseksou, Marie-Laure Boillot,\*

### Figures

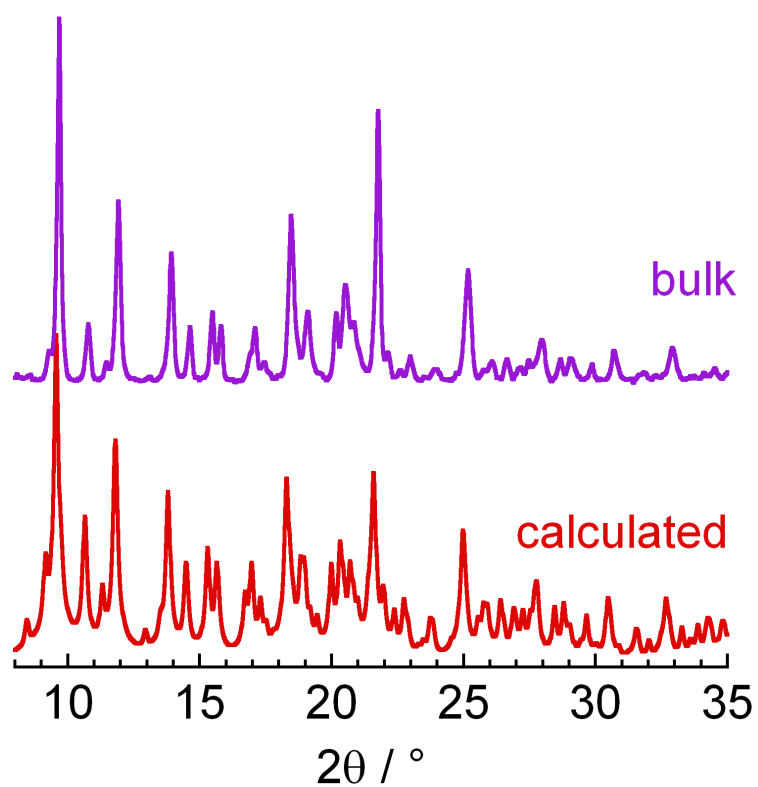


Figure S1: Room temperature powder X-ray diffractogram of  $[\text{Fe}^{\text{III}}(\text{3-MeO-SalEen})_2]\text{PF}_6$  in the  $8\text{-}35^\circ$  range (bulk) and diffractogram calculated from the structure at 293 K determined by single crystal X-Ray diffraction (in reference 20).

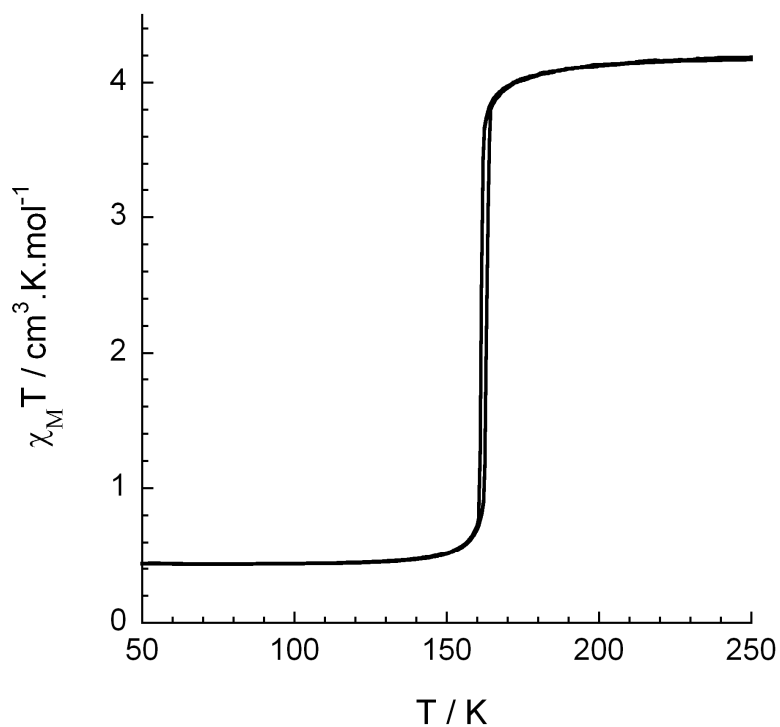


Figure S2: Temperature dependence of the  $\chi_M T$  product ( $\chi_M$  = molar magnetic susceptibility,  $T$  = temperature) for the powdered sample of  $[\text{Fe}^{\text{III}}(3\text{-MeO-SalEen})_2]\text{PF}_6$ . (From reference 20)

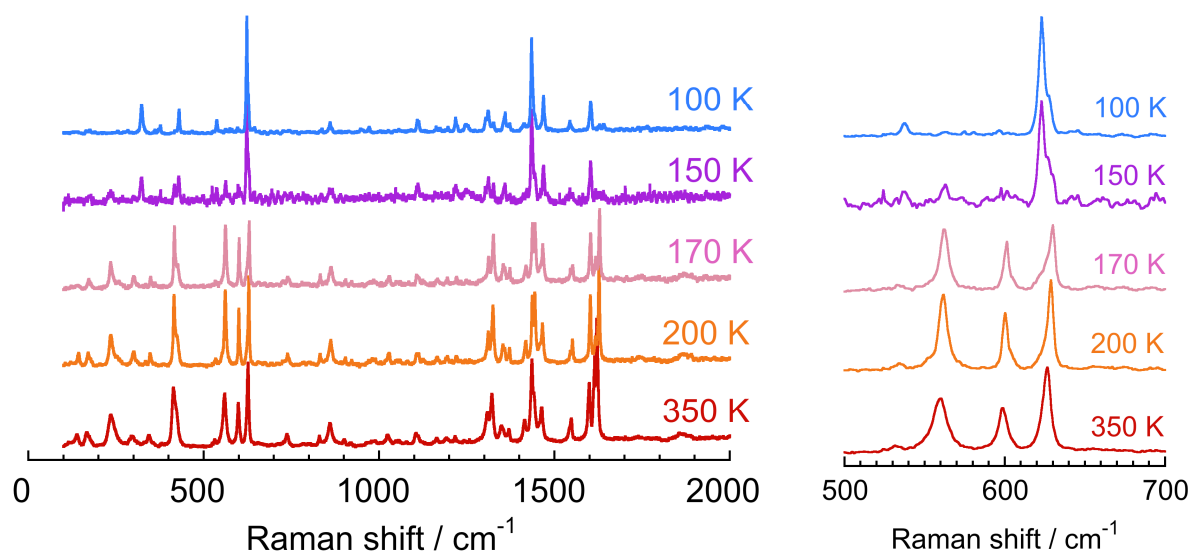


Figure S3: Variable temperature Raman spectra of  $[\text{Fe}^{\text{III}}(3\text{-MeO-SalEen})_2]\text{PF}_6$  in the form of a microcrystalline powder (bulk). Expansion of the Raman spectra in the 500-700  $\text{cm}^{-1}$  range

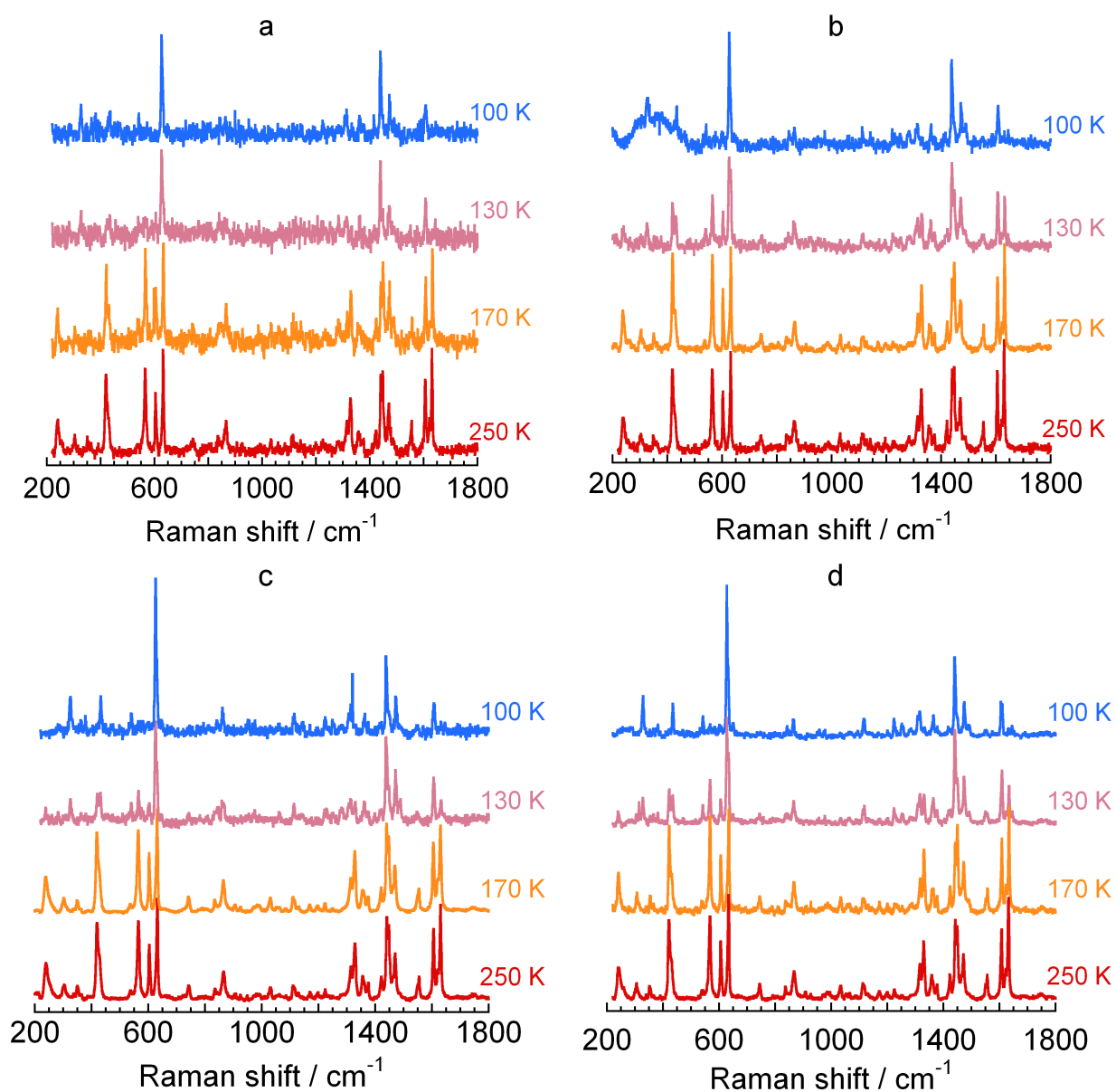


Figure S4: Variable temperature Raman spectra of the composites containing 7.5  $\mu\text{m}$  (a), 3  $\mu\text{m}$  (b), 1  $\mu\text{m}$  (c) and 18 nm (d) long particles of  $[\text{Fe}^{\text{III}}(3\text{-MeO-SalEen})_2]\text{PF}_6$ .

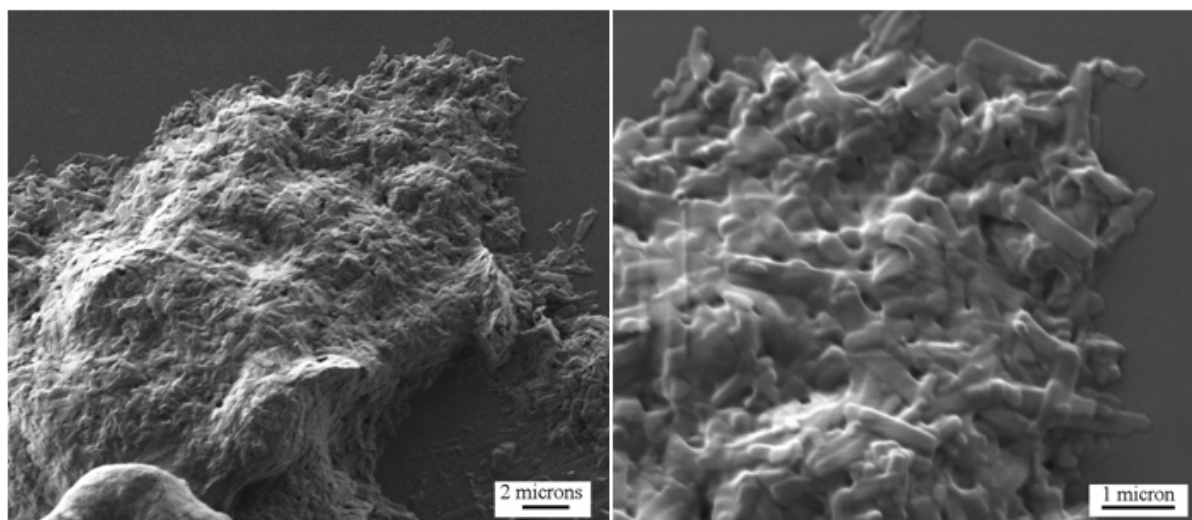


Figure S5: SEM images of the 1  $\mu\text{m}$  long microparticles (sample **b**) embedded in the PEG polymer.

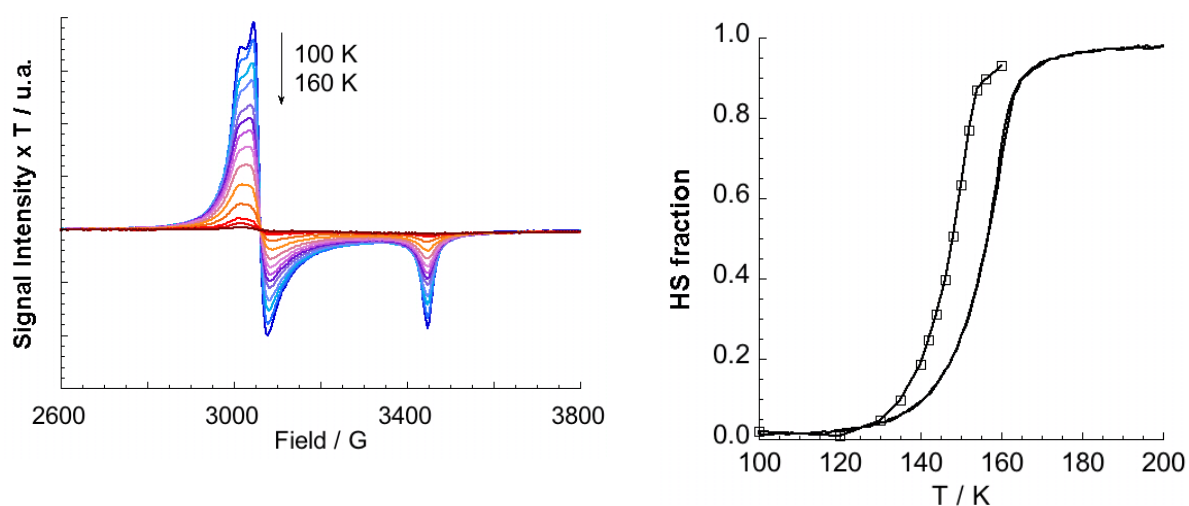


Figure S6: (left) The X-band EPR signal registered as a function of temperature for the 7.5  $\mu\text{m}$  microcomposites (sample **a**,  $T = 100, 120, 130, 135, 140$  K and then every 2 K up to 160 K). (right) The HS fraction vs. temperature plot corresponding to spin-transition species analyzed from the LS EPR signal ( $\square$ ) and magnetic data ( $\text{—}$ ).